HYDRAULIC LIME MORTAR IN THE AMBIT OF STONE RESTORATION: EVALUATION OF APPLICABILITY

Stephan Kröner[1], María-Teresa Doménech-Carbó[1] and Xavier Mas-Barberà[2]
Instituto Universitario de Restauración del Patrimonio de la Universidad Politécnica de Valencia
[1]Laboratorio de análisis físico-químicos y control medioambiental de Obras de Arte
[2]Taller de conservación y restauración de elementos escultóricos y ornamentales

CONTACT AUTHOR: Stephan Kröner, ustephan@upvnet.upv.es

ABSTRACT: *This study presents the results of the applicability of hydraulic lime mortars in the ambit of stone conservation and restoration. Historical buildings, as well as sculptures or ornamental artworks exposed to environmental influences, composed by natural stone materials suffer severe alteration / degradation in the course of time. On this account, the physico-chemical properties of hydraulic lime mortars have been compared with those of two calcarenitic rocks (Barxeta and Bateig azul), found in historical Valencian monuments.*
A systematically analytical procedural method was established on a series of test specimens in order to prove compatibility / replaceability of limestones. The specimens were subjected to standard accelerated physical-chemical ageing tests. Compressive and flexural strength tests have been performed on the mortars and the stone material in order to determine the physical degradation. Alteration by chemical attack was simulated by the exposure in a SO_2 pollutant chamber and salt crystallisation test. The experiments performed show that the applied mortars have on one hand similar physical resistance and on the other hand present higher chemical resistance properties, especially against salt crystallisation in comparison to the natural stones and therefore might be of special interest for replicas.

KEYWORDS: hydraulic lime mortar, physico-chemical properties, accelerated ageing, SEM/EDX, Barxeta, Bateig azul

1. INTRODUCTION

The appropriate selection of the mortar in the ambit of stone restoration and conservation of historical monuments is essential at the time of intervention. The physical-chemical properties of a mortar should match as close as possible to those of the unaltered original stone material (masonry, sculpture, ornament etc.). This could be considered as a fundamental requirement in order to avoid incompatibilities of the "host rock" with the repair/ replacement mortar. Resin bound mortars, e.g., show excellent results for mechanical behaviour and also satisfactory resistance to different alteration agents (Roig-Salom et al., 2003; Mas-Barberà 2005), but employed within construction material of completely different physico-chemical behaviour a converse effect might occur and deterioration can be accelerated (Maravelaki-Kalaitzaki et al., 2005).

Hydraulic lime and aerial lime based mortars have been used for centuries as binder for construction purposes, while in the last century replacement by cement based mortars came into vogue. Primarily faster setting, higher mechanical resistance and economical reasons argued in favour cement mortar employment instead of the traditional mortars. However, high soluble salt contents, low flexibility resistance and low water permeability discarded nowadays application in historical monuments and lead to a "rediscovery" of lime based mortars (Lanas and Alvarez, 2003; Moropoulou et al., 2005; Arandigoyen and Alvarez, 2007).

Limestone is largely employed in cultural heritage. In these rocks, accessory minerals (clay minerals, iron oxides, quartz content, etc.) as well as physical properties such as porosity (intracrystalline, interparticle, open, etc.) and degree of compaction determine the resistance against alteration processes.

Hydraulic lime binder can normally be obtained by burning limestone that contains clay minerals or other impurities at a temperature above 900°C (Maravelaki-Kalaitzaki et al., 2005; Cowper, 2000).

Calcium carbonate is transformed to calcium oxide and carbon dioxide. In a second step, water is added, resulting in slaked lime $Ca(OH)_2$, which is the bases of every hydraulic lime binder. While the binder mainly determines the cohesive properties of the mortar, the particle size distribution of the aggregate, being the major component of the mortar, influences the mechanical properties of the mortar (Roig-Salom et al., 2003; Lanas et al., 2004). In this investigation the commercial Ledan C30 has been used as binder and crushed *Bateig*, respectively *Barxeta* stone has been added as aggregate.

In this study, properties of two limestones from the Valencian region (Spain), *Bateig azul* and *Barxeta*, and the corresponding hydraulic lime mortars have been subjected to standard acceleration tests in order to determine whether the latter ones could be used for restoration purposes.

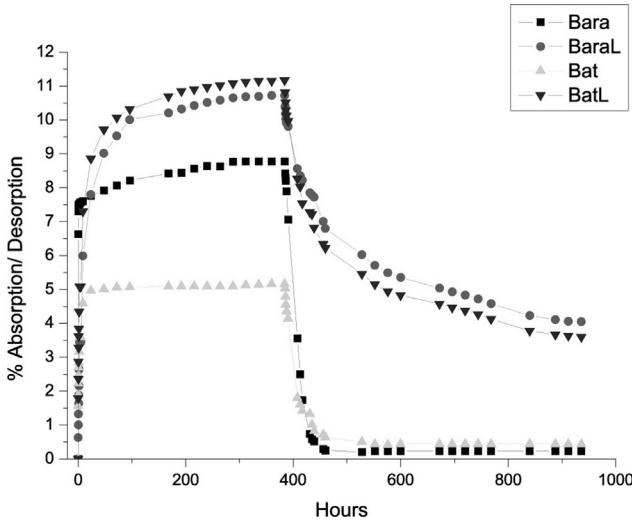

Figure. 1. Weight gain/loss in % of the test specimens subjected to immersion in water until no weight variation <0,1%, followed by a drying period at room temperature (20°C) presented in a absorption-desorption diagram

2. STONE MATERIALS

Two limestones, employed in the monumental heritage of the Valencian Community (Spain), have been analysed. The foraminiferal-rich pelagic *Bateig azul* limestone, extracted from the quarry of the Bateig hill (Alicante, SE Spain), is composed by fine-grained sandy calcite $CaCO_3$ (biosparite), containing angular quartz grains and glauconite (phyllosilicate mineral). Porosity is very abundant, uniform and interconnected, presenting pores without recrystallised calcite.

The second limestone, *Barxeta*, has been extracted from a quarry around 50 km south of Valencia at the limit of the external Pre-Betic and the SE Iberian mountain range. The *Barxeta* limestone is a detrital sedimental rock, composed of mainly calcite and minor angular shaped quartz, clay minerals and limonite (hydrated iron oxide-hydroxide, $FeO(OH)\cdot nH_2O$). The *Barxeta* limestone is courser grained, also sparitic (63µm-2mm), but intergranular cohesion is lower.

The X-ray diffraction of the two stones reveals the presence of calcite and quartz as major components and confirms observations from the petrographical microscope.

3. EXPERIMENTAL

3.1 Mortar preparation

The special hydraulic lime binder Ledan C30 has been used to prepare the mortar specimens. The elaborated binder/aggregate ratios for both mortars, the *Bateig azul* (BatL) and the *Barxeta* (BaraL), was 1:2. The mortar pastes were obtained using the amount of water required to achieve normal consistency and a good workability (Table 1, presents these results together with the amount of water added). Eighteen prisms of 50x50x50 mm for physical-chemical property characterisation (6 absorption-desorption, 6 freezing-thawing, 6 salt crystallisation) and six samples (160x40x40 mm) for flexural and compressive strength tests were prepared using moulded casts and demoulded 48h later.

	<0.25 mm	0.25-0.42mm	Ledan C30	Water
Bateig azul	11.0	44.0	27.5	17.6
Barxeta	44.9	11.2	28.1	15.7

Table. 1. Composition of hydraulic mortars in weight %. Aggregate/ binder =2:1

3.2 Instrumentation

3.2.1. Physical properties determination

For a physical characterisation, complementary analyses have been performed, like hydrostatic weight and water saturation in order to determine real density and open porosity.

Water absorption-desorption test was carried out following the EN-196-1/996 norm recommendation on the test specimens.

Mechanical evaluation on the mortar specimens was performed with the three-point flexural test after the EN-196-1/996 norm using a loading rate of 4 mm/min. Compression strength test was carried out on the two fragments of each specimen resulting of the previous flexural test and the rate of loading was 10 mm/min.

3.2.2. Mineralogical and chemical characterisation

X-ray powder diffraction (XRD) analysis was carried out using a Siemens DMP 2000 X-ray diffractometer with CuKα radiation at the wavelength of 1.5405 Å.

A representative amount of a fresh rock sample obtained directly from the quarry was crushed by hand using an agate mortar and pestle for Fourier transform infrared spectroscopy (FTIR) analysis. IR absorption spectra were performed in the attenuated total reflectance mode (ATR) with a Vertex 70 Fourier transform infrared spectrometer and with a fast FR-DGTS (fast recovery deuterated triglycine sulphate) temperature-stabilised coated detector. The number of co-added scans was 32; resolution: $4cm^{-1}$.

Morphological examination and chemical composition of the mortars and limestones were obtained by using a Jeol JSM 5410 scanning Electron Microscope, operating with a Link–Oxford–Isis microanalysis system. The analytical conditions were: 20 kV accelerating voltage, 2×10^{-9}A beam current and 15 mm working distance. The polished samples were carbon-coated to eliminate charging effects.

3.2.3. Physical, chemical and resistance tests

Resistance against accelerated freezing-thawing cycles was determined for natural stones as well as for corresponding mortars. Freezing cycle ageing: this consisted of 48 cycles in which the test specimens were frozen for 6 h at -15 °C and then they were immersed in water for 18 h at 0 °C (RILEM 1980). Samples were weighed at the beginning, during and at the end of the test.

	Real Density (g/cm^3)	Standard deviation	Open porosity %	Standard Deviation
Bateig	2.53	0.01	11.53	0.31
Mortar Bateig	2.06	0.02	13.21	0.05
Barxeta	2.21	0.01	23.11	1.91
Mortar Barxeta	1.98	0.02	8.09	0.06

Table. 2. Properties of the natural stones and hydraulic lime based mortars

	Weight Loss (-) or gain (+) in %, salt crystallisation ageing	Standard deviation	Weight Loss (-) or gain (+) in %, freezing cycle ageing	Standard deviation
Bateig azul	-56	15	-0.17	0.03
Mortar Bateig	+2.47	0.05	1.01	0.15
Barxeta	-20	7	-0.81	0.07
Mortar Barxeta	+2.31	0.08	1.75	0.05

Table. 3. Stone/ mortar decay due to salt crystallisation and freezing thawing cycles

Standard Salt crystallisation ageing (RILEM 1980): this consisted of 15 cycles in which the test specimens were immersed for 4 h in a saturated sodium sulphate solution (14% $Na_2SO_4 \cdot 10H_2O$). They were then dried for 19 h at 60°C and finally cooled for 3 h at 20 °C and weighted.

The accelerated ageing test by SO_2 was performed in a SO2 saturated pollutant chamber after Kesternich (DIN 50.018). It consists in drying the test specimens at 60°C until obtaining a non-varying weight. Then 7 cycles (168h) of accelerated ageing have been carried out: 8h at 40°C with 2 l/g SO_2 concentration and 100% RH followed by 16h drying at room temperature. After the test, the specimens have been weighted and analysed by the scanning electron microscope coupled with X-Ray microanalysis (SEM/EDX).

4. RESULTS AND DISCUSSION

4.1. Physical properties determination

The density of calcite is 2.71 g/cm^3, thus limestones with no porosity result in density log values close to 2.71 g/cm^3, while limestones with ~10% porosity have density values around 2.54 g/cm^3, respectively limestone with 20% porosity values around 2.37 g/cm^3 (d=2.71(g)/cm^3 ×(100-%porosity)/100+1×(%porosity)/100). The density log values for both natural limestones confirm these predictions. Open porosity values for the Bateig Ledan mortar are very similar, while the Barxeta Ledan mortar has much lower porosity values. Real density values for the mortars cluster around 2 g/cm^3, being of special interest for architectural use where the load might be important (Table 2).

Accelerated ageing by freezing cycles resulted in no significant weight changes neither for mortar nor for natural stones (Table 3)

4.2. Mineralogical and chemical characterisation

Mineralogical and chemical characterisation of the rocks and restoration mortars was determined by three 'classical' analytical techniques: XRD, FTIR and SEM/EDX. XRD is often used to determine the mineralogical composition and degree of crystallinity as well as qualitative and quantitative phase analysis. X-Ray powder diffraction patterns are illustrated in Figure 2. Both limestones show typical d-spacings for calcite, however intensity in the *Barxeta* stone is higher and sharpness of calcite peaks is stronger, indicating higher crystallinity of calcite. In both rocks XRD reveals quartz as second major component, whereas in the *Bateig azul* stone additionally small amounts of glauconite (iron-bearing phyllosilicate) and dolomite $CaMg(CO_3)_2$ were detected. In order to determine hydraulic lime

IR absorption bands Wavenumbers (cm^{-1})		Assignment
Limestones		
Barxeta	Bateig	
713	712	v_4-Symmetric CO_3 deformation, calcite
n.o.	728	v_4-Symmetric CO_3 deformation, dolomite
781	780	Qtz-doublet
799	797	Qtz-doublet
872	873	v_2-Asymmetric CO_3 deformation
918	919	OH-deformation bands (AlAlOH)
1032	1022	Si-O stretching bands
1089	1085	Si-O stretching bands
1170	n.o.	Si-O stretching bands, quartz
1406	1414	v_3-Asymmetric CO_3 stretching
1796	1798	v_1+ v_4, calcite
2512	2513	$2v_2$+ v_4, calcite

Table. 4.Main IR absorption bands (**V**) of infrared bands of limestones and assigned modes

IR absorption bands Wavenumbers (cm^{-1})		Assignment
Hydraulic lime mortar		
Barxeta	Bateig	
712	712	v_4-Symmetric CO_3 deformation
n.o.	779	Qtz-doublet
n.o.	799	Qtz-doublet
873	874	v_2-Asymmetric CO_3 deformation
968	973	v_3, SiO_4, C-S-H
1002	1010	Si-O stretching bands, C-S-H
1085	1082	Si-O stretching bands, quartz
1407	1410	v_3-Asymmetric CO_3 stretching
1638	1641	deformational vibration H–O–H, C-S-H
1797	1798	v_1+ v_4, calcite
2509	2513	$2v_2$+ v_4, calcite
~3400	~3400	$v_{1\text{-}3}$, H_2O, C-S-H
3639	3642	v, OH^- free CH, portlandite

Table. 5. Main IR absorption bands (**V**) of infrared bands of mortars and assigned modes

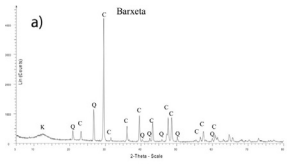

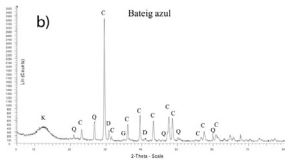

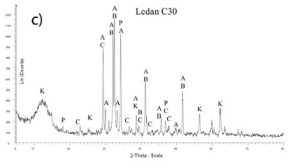

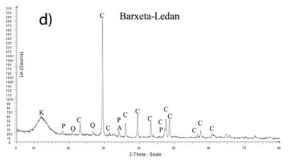

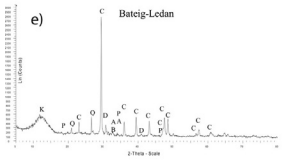

Figure. 2. Powder XRD patterns of the Barxeta (a) and Bateig azul (b) stones, the hydraulic lime mortar Ledan C30 (c) and the corresponding mortars (d and e). A: Alite; B: Belite; C:Calcite; D: Dolomite; G: Glauconite; K: Kaolinite; P: Portlandite; Q: Quartz

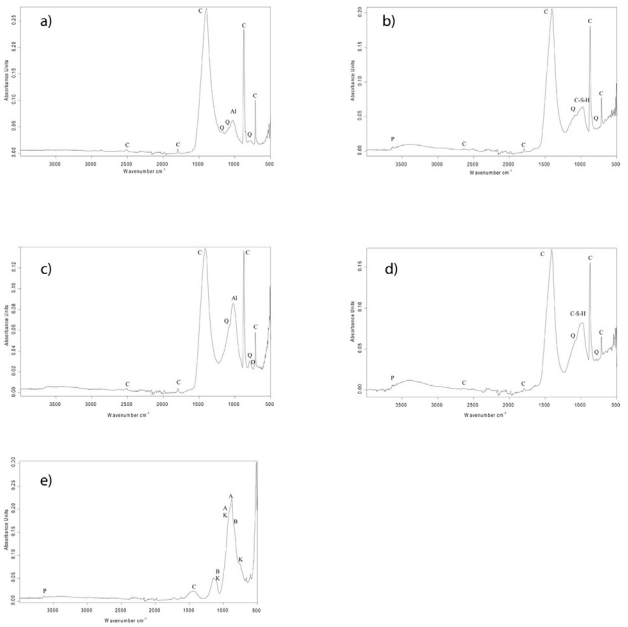

Figure. 3. IR absorption spectra. a) Barxeta, b) Barxeta Ledan, c)Bateig azul, d) Bateig Ledan, e) Ledan. A: Alite; Al: Aluminum silicate; B: Belite; C: Calcite; C-S-H: Calcium-Silicate-Hydrate, D: Dolomite; K: Kaolinite; P: Portlandite; Q: Quartz

binder composition XRD of Ledan C30 was carried out. Tricalcium silicate Ca_3SiO_5 (alite), dicalcium silicate Ca_2SiO_4 (belite) and kaolinite $Al_2Si_2O_5(OH)_4$ are major constituents and calcite $CaCO_3$ and portlandite $Ca(OH)_2$ minor admixtures. The restoration mortars exhibit XRD patterns of calcite and quartz from the host rocks.

FTIR patterns of the *Barxeta* and *Bateig azul* stones and their corresponding restoration mortars together with the spectra of the pure hydraulic lime binder are shown in Figures 3a-e and identification of the IR absorption bands and assigned modes presented in Tables 4 and 5.

The analysis of both rocks, *Barxeta* and *Bateig azul*, resulted in a quite similar spectrum with typical calcite carbonate $CaCO_3$ absorption bands at 713 (712), 872 (873), 1406 (1414), 1796 (1798) and 2512 (2513) cm^{-1}. These bands are in good agreement with those reported in the literature (Gunasekaran et al., 2006; Adler and Kerr, 1963; Shoval, 2003). The minor shift position of the v3 band to lower wavelengths might by due to impurities like trace metal elements and/or the presence of clay minerals. Accessory minerals like quartz (Qtz-doublet at 780-790 and Si-O stretching at ~1085) and aluminium silicates (Si-O stretching at ~1032, AlAlOH stretching at ~918). Additionally a small peak at 728 cm^{-1} for the *Bateig azul* stone confirms the X-Ray diffraction results pointing to small presence of dolomite within the natural stone.

The combination of XRD and FTIR analysis is a useful tool for the evaluation of hydraulic lime mortars. Apart from the CO_3^{-2} absorption bands, coin cidently with the rock values, portlandite $Ca(OH)_2$ and calcium-silicate-hydrate (C-S-H) could be identified. Typical OH-stretching at ~3640cm^{-1} corresponding to Ca–OH in portlandite and a broad absorption around 3410 cm^{-1} for hydrates (C-S-H), deformational vibration H-O-H at ~1640 cm^{-1} and Si-O stretching at ~1000 and 970 cm^{-1} for C-S-H was detected. In particular, the broad absorption band between 970-1010 cm^{-1} is characteristic for C-S-H (Saikia et al., 2002; Maravelaki-Kalaitzaki et al., 2005; Varas et al., 2005; Lavat 2008). Again, IR analysis of pure hydraulic lime mortar for providing supplementary information to XRD was performed. The principal constituents alite, belite and portlandite, and kaolinite and calcite as minor components could be identified.

Combining both, mortars and binder IR spectra the following reactions can be explained:

	Flexural strength (MPa)	Standard deviation	Compression strength (MPa)	Standard deviation
Bateig azul	8.1	0.3	39.1	0.1
Mortar Bateig	7.6	0.2	29.7	0.3
Barxeta	7.1	0.4	32.8	0.5
Mortar Barxeta	8.2	0.4	29.7	0.6

Table. 6. Comparison flexural and compressional strength of original stone with lime mortar

Alite+water: $2Ca_3OSiO_4 + 6H_2O \rightarrow 3CaO.2SiO_2.3H_2O + 3Ca(OH)_2$

Belite + water: $2Ca_2SiO_4 + 4H_2O \rightarrow 3CaO.2SiO_2.3H_2O + Ca(OH)_2$

These reactions produce calcium silicate hydrates and portlandite, while in a second step, portlandite is transformed to calcium carbonate $CaCO_3$ (van Balen and van Gemert, 1994; van Balen , 2005):

$CO_2 + H_2O \rightarrow H_2CO_3$

$Ca(OH)_2 + H_2CO3 \rightarrow CaCO_3 + 2H_2O$

In the IR spectra of mortars displacement of Si–O bands for tricalcium silicate (C_3S) and dicalcium silicate (C_2S) at 911-846 cm^{-1} toward a higher wavenumber (ca. 970 cm^{-1}), as a consequence of a change in the environment of Si–O by formation of Si–O–H bonds can be observed(Saikia et al., 2002; Lavat et al., 2008).

Furthermore, the presence of portlandite within the mortars indicate, that complete carbonation was not achieved after one year (Maravelaki-Kalaitzaki et al., 2005).

4.3. Compression and flexion strength

It can be observed that for the flexural essays the results for both hydraulic mortars converge very closely the natural stones. Regarding the compression strength for the Barxeta mortar (BaraL) the resistance is quite similar to the natural stone, while the obtained

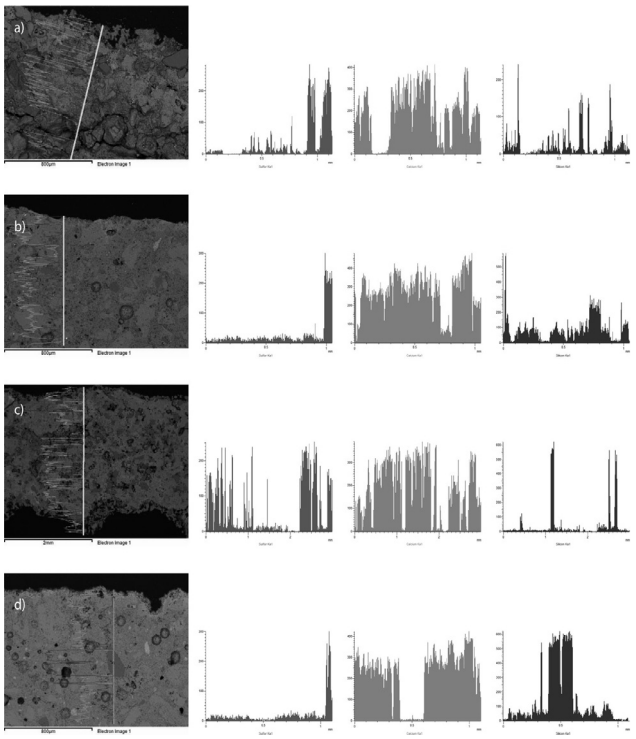

Figure. 4. Electron microscope images and profiles after SO_2 saturated pollutant chamber test.Element profiles indicated by yellow line. Width of images 1,6 mm (A, B and D) and 4mm (C). Profiles: red: Sulfur; green: Calcium; blue: Silicon. A) SEM image of the natural Bateig azul stone. Penetration depth of sulphur (gypsum formation) ≈0,8 mm. B) SEM image of the hydraulic mortar Bateig (Ledan). Penetration depth of sulphur ≤0,1mm. C) SEM image of the natural Barxeta limestone. Penetration depth of sulphur ≥1,5 mm. D) SEM image of the hydraulic mortar Barxeta (Ledan). Penetration depth of sulphur ≤0,1mm

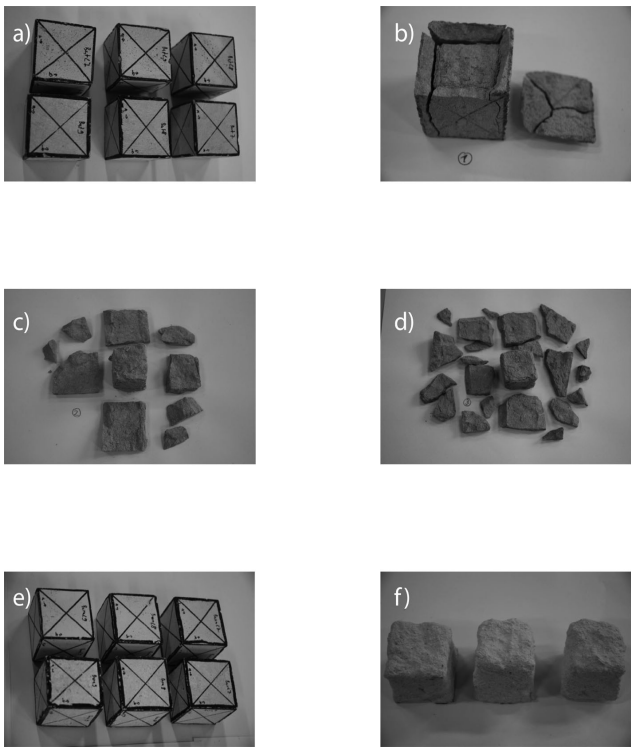

Figure. 5. Test specimens subjected to salt crystallisation test. a+e) Bateig azul and respectively Barxeta before test. b-d) Bateig azul after test. Homogenous layer detachment can be clearly observed. f) Barxeta limestone after test. Loss of grain cohesion causes erosion of stone material

	Cycle O (g)	Cycle 7 (g)	Weight gain (%)
Bateig azul	0.9518	0.9971	4.76
Mortar Bateig	0.6722	0.7013	4.33
Barxeta	0.8536	0.8911	4.39
Mortar Barxeta	0.7248	0.7580	4.58

Table.7. SO_2 saturated pollutant chamber test after Kesternich (DIN 50.018)

value for the Bateig mortar (BatL) is below the original one (Table 6). The Bateig repair mortar exhibits lower compressive strength than the stone, but the value lies in acceptable ranges since the repair mortars exhibit similar modulus of elasticity to the stone.

4.4. SO2 saturated atmosphere

This test simulates the degradation of the historical architecture affected by atmospheric pollution. Since the industrial revolution starting end of the 19th century, deterioration of carbonate rocks (limestones, marbles and dolostones) by pollutants such as sulphur dioxide, generated by combustion of fossil fuels, is getting in the focus of greater interest. Black crust formation is attributed to combination of two processes: acid rain transforms calcite to gypsum (dolostones: dolomite $CaMg(CO_3)_2$ to gypsum and epsomite $MgSO_4 \cdot 7H_2O$) and the dark aspect is due to dust capture of the newly formed gypsum. In particular monuments located in urban areas are affected by this degradation process.

In this essay it had observed that all specimens exhibit an increase of weight (4-5%) due to sulphate attack processes (SO_2(g)). Nevertheless the penetration depth of the sulphur, more precisely the gypsum concentration, differs very strongly between the natural stone and the repair mortars. While the hydraulic mortars have only been attacked at the surface (≤0,1 mm), the alteration by SO_2 is more severe within the natural stones (1-2 mm) as it can be deduced from the diagrams shown in Figures 4a-d.

4.5. Salt crystallization resistance

Alteration of natural stones by salt crystallisation is one of the mayor causes for material deterioration. Precipitation of soluble salts within the porous materials can result in severe damages within historical buildings (Evans, 1970; Ruiz-Aggudo, 2007). In architectural stones or mortars, salts can either emanate from ascending moisture derived from ground water or induced by atmospheric pollution at a higher elevation beyond the reach of moisture (Winkler and Wilhelm, 1970; Winkler and Singer, 1972).

The disintegration of stones or concrete is governed by the exert pressure due to salt crystallisation in capillary tubes. Salt crystallisation depends on supersaturation of the salt in the liquid, while the degree of damage relies on pore size, pore distribution, intragranular cohesion and the order of stress applied to the enveloping pore surfaces (Scherer, 2004). Supersaturation in the liquid can be caused by evaporation processes or temperature changes. The crystallisation stress P can be calculated as follows, known as Correns's law (Correns, 1949):

$$p=(Rg\ T)/V_C\ \ln(Q/K)$$

P: pressure exerted by growing crystal; R: gas constant 8.314472 J mol^{-1} K^{-1}; T: absolute Temperature ºK; V_c: molar volume of the crystal; Q: solubility product; K: equilibrium solubility for a macroscopic crystal.

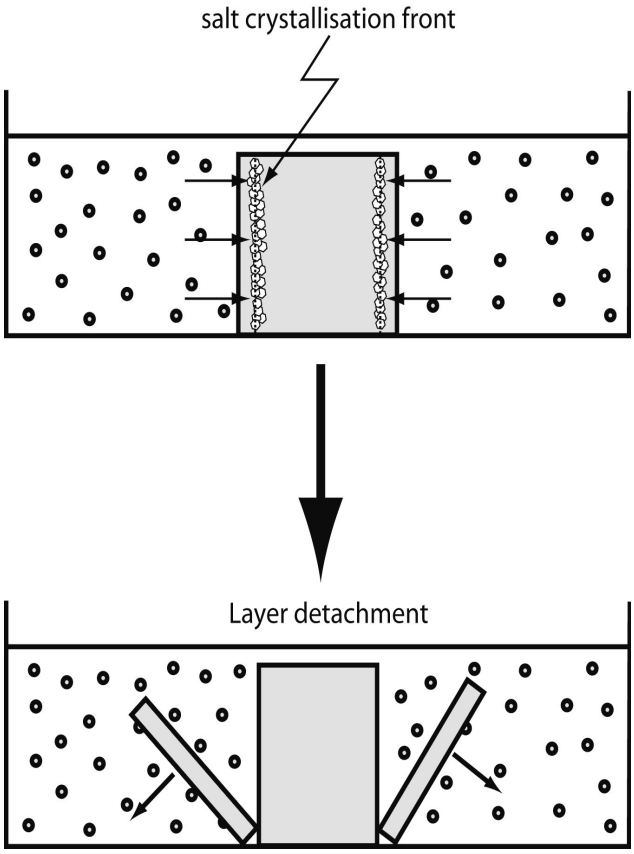

Figure. 6: Sketch simplifying deterioration process of the Bateig azul stone subjected to salt crystallisation test in a $NaSO_4$ saturated water solution. Crystal growth at high supersaturation over a large part of the test specimens and the stress fields propagates strength limiting flaws, producing homogeneous layer detachment

The crystallization stress is lower in larger pores and Scherer and Benavente et al. (Scherer, 1999; Scherer, 2004; Benavente et al., 1999) evidenced that fracture obviously is not caused by crystallisation in a single pore, but requires growth of the crystal through a region of the body comparable in size to the strength controlling flaws. The ratio Q/K is the supersaturation ratio, or the degree the solution is oversaturated with respect to some solid phase.

Sodium sulphate is one of the most destructive salts and the standard salt experiment (RILEM 1980) has been carried out due to its particular interest. In a cyclic test, the specimens were immersed in a sodium sulphate solution and then dried (15 times). In the pores of the mortars and rocks crystallises accordingly mirabilite NaSO4·10H2O (wetting cycle) and thenardite $NaSO_4$ (drying cycle). The case of the *Bateig azul* stone is of special interest because severe deterioration occurs in the wetting cycle and at the end of the test, submerged to tap water. As stated by several authors (Correns, 1949; Doehne 1994; Flatt, 2002; Flatt and Scherer, 2002; Thaulow and Sahu, 2004;) this is probably not due to hydration of thenardite to mirabilite ($NaSO_4+10H_2O \rightarrow NaSO_4 \cdot 10H_2O$), instead complete dissolution of thenardite and new precipitation of mirabilite in a highly supersaturated liquid is taking place and the resulting volume/stress increase might be responsible for the stone alteration.

While the two repair mortars did not experienced any decomposition and preserved the original cubic shape (only weight gain of about 2-3%), both limestones have been deteriorated severely. Nevertheless two different disintegration processes can be observed: Homogenous layer detachment (about 8mm thickness) within the *Bateig azul* stone versus loss of grain cohesion within the *Barxeta* limestone (Table 4, Figures 5a-f).

The homogenous layer detachment might be explained by the following successive processes:

a) Water penetrates the porous network quickly due to capillarity forces

b) Dissolution of thenardite is faster than reprecipitaction of mirabilite

Figure. 7. a) Original gothic cross with lichen, b) replica in 2006 and c) replica in 2009. Note: only the cross was replaced, while the column has been retained unchanged. Increase of biological attack of the column whereas the mortar seems not to be affected

These conditions lead to crystal growth at high supersaturation over a large part of the test specimens and the stress fields can propagate strength limiting flaws (Ver figura 6). The mechanical action of crystallisation pressure on the surface of the pores produces an increase in the number of pores, connected pores and channel porosity (Scherer , 1999; Benavente et al., 1999; Flatt, 2002).

4.6. Real case application

The joint mortar replica of the gothic cross '*Creu de Terme'* located on a cemetery in the *Pobla LLarga* village (about 50 km southwest of Valencia town, Spain) was prepared with Ledan C30 in the year 2006. The original cross, made of biocalcarenitic stone, exhibited severe damages and it was opted for a total replacement, while the original piece was relocated in a museum under controlled conditions. The mortar was prepared as described above, and the aggregate/ binder ratio was 2:1.

Figure 7 shows the cross a) before, b) directly after and c) three years after the intervention. It can be observed that, while slow deterioration of the column is still going on (biological attack of lichen etc.), the hydraulic lime replacement mortar is neither affected by salt crystallization nor by biological deterioration. In order to prove carbonation state, a FTIR analysis of the mortar after 3 years was carried out.

Portlandite was not observed, leading to the conclusion that the carbonation process of the hydraulic lime Ledan C30 is completed in between one to three years.

5. CONCLUSIONS

a) The hydraulic lime mortars show similar values for flexural and compression strength to the original stones. This implies good compatibility with the natural stone.

b) Salt crystallisation resulted in two different types of disintegration of the natural stone, due to the difference of pore sizes and intragranular cohesion within these two limestones. Physical stress resulting from salt crystallisation close to the surface leads to a layer detachment within the more compact *Bateig* stone all at once, while lower grain cohesion in the Barxeta limestone resulted in a slowly and constantly grain by grain extraction. Additionally, these two stones show little resistance to attack by SO_2. On the other hand the hydraulic mortars improve clearly the resistance against SO_2 and Na-sulphate attack and do not show any disintegration phenomena.

It can be concluded, that the properties of the applied hydraulic lime binder fulfil satisfactorily the desired requirements for whole replicas in the ambit of stone restoration of these two limestones. However, the durability of the stones towards salt weathering is significantly lower than that of the mortar.

This means that in the event that the stones are subjected to salt weathering, the damage will be concentrated in the stone, which could be detrimental in a real case scenario where the hydraulic mortar is used for repair in a stone structure.

ACKNOWLEDGMENTS

Financial support is kindly acknowledged to the Spanish MEC I+D+I Project CTQ 2005-09339-L03-01, also supported by FEDER founds and the grant for stays of doctors in research centres of excellence in the Valencia Community (Generalitat Valenciana I+D program, DOGV 17/11/2006).

The authors would like to thank for the facilities using and the technical supervisors Dr. José Luis Moya López and Mr. Manuel Planes Insausti of the Scanning Electron Microscopy Service of the UPV as well as María José Pelufo of the Construction Engineering and Civil Engineering Project Department.

APPENDIX

Ledan C30.

Tecno Edile Toscana. Prodotti e tecnologie per el restauro.

Via Monti Lepini, 14

04100 Latina

e-mail: ledan@tecnoediletoscana.com

Italy

BIBLIOGRAPHY

Adler, H. H. and Kerr, P.F. (1963): 'Infrared absorption frequency trends for anhydrous normal carbonates', *The American Mineralogist* **48** 124-137

Arandigoyen, M., Alvarez, J.I., (2007): 'Pore structure and mechanical properties of cement–lime mortars', *Cement and Concrete Research* **37** 767–775

Benavente, D., García del Cura, M.A., Fort, R., Ordóñez, S., (1999): 'Thermodynamic modelling of changes induced by salt pressure crystallisation in porous media of stone', *Journal of crystal growth* **204** 168-178.

Correns, C.W., (1949): 'Growth and dissolution of crystals under linear pressure', *Discuss. Faraday Soc.* **5** 267– 271.

Cowper, A.D. (2000): Lime and lime mortars, Donhead Publishing Ltd., Dorset, 81 pages

Doehne, E., (1994) :'*In situ* dynamics of sodium sulfate hydration and dehydration in stone pores: observations at high magnification using the environmental scanning electron microscope', in: V. Fassina, H. Ott, F. Zezza (Eds.), *III Int. Symp. Conservation of Monuments in the Mediterranean Basin*, Venice, Soprintendenza ai beni artistici e storici di Venezia, Venezia, 143– 150.

Evans, IS, (1970): 'Salt crystallisation and rock weathering: A review', *Revue Géomorphologie Dynamique* **19**, 153-177.

Flatt, R.J., (2002): 'Salt damage in porous materials: how high supersaturations are generated', *Journal of Crystal Growth* **242** 435–454

Flatt, R.J., Scherer, G.W., (2002) 'Hydration and crystallization pressure of sodium sulfate: a critical review', in: P.B. Vandiver, M. Goodway, J.L. Mass (Eds.), Materials Issues in Art & Archaeology VI, MRS Symposium Proc., vol. 712, Materials Res. Soc., Warrendale, PA, 29– 34.

Gunasekaran, S., Anbalagan, G., Pandi, S., (2006): 'Raman and infrared spectra of carbonates of calcite structure', *Journal of Raman Spectroscopy* **37** 892-899.

Lanas, J., Alvarez, J.I., (2003): 'Masonry repair lime-based mortars: Factors affecting the mechanical behaviour', *Cement and Concrete Research* **33** 1867–1876

Lanas, J., Perez Bernal, J.L., Bello, M.A., Alvarez Galindo, J.I., (2004): 'Mechanical properties of natural hydraulic lime-based mortars', *Cement and Concrete Research* **34** 2191-2201.

Lavat, A. E., Trezza, M. A., Poggi, M., (in press 2008): 'Characterization of ceramic roof tile wastes as pozzolanic admixture', *Waste Management*

Maravelaki-Kalaitzaki, P., Bakolas, A., Karatasios, I., Kilikoglou, V., (2005): 'Hydraulic lime mortars for the restoration of historic masonry in Crete', *Cement and Concrete Research* **35** 2191-2201.

Mas i Barberà, X. (2006): *Estudio y caracterización de morteros compuestos, para su aplicación en intervenciones de sellados, reposiciones y réplicas, de elementos pétreos escultórico-ornamentales,* PhD thesis, Universidad Politécnica de Valencia, Departamento de Conservacion y Restauracion de Bienes, 413pp.

Moropoulou, A., Bakolas, A., Moundoulas, P., Aggelakopoulou, E., Anagnostopoulou, S., (2005): 'Strength development and lime reaction in mortars for repairing historic masonries', *Cement & Concrete Composites* **27** 289–294

Norma EN-196–1/996: *Recommended tests to measure the mechanical properties of cements*.

RILEM (1980): *Recommended tests to measure the deterioration of stone and to assess the effectiveness of treatment methods, Commission 25-PEM: Protection et Erosion des Monuments*. Essai N° V.3: Tenue a gel, 238–244

RILEM (1980): *Recommended tests to measure the deterioration of stone and to assess the effectiveness of treatment methods, Commission 25-PEM: Protection et Erosion des Monuments.* Essai N° V.1a: Cristallisation par immersion totale, 234–236

Roig-Salom, J-L., Doménech-Carbó, M-T, de la Cruz-Cañizares, J., Bolívar-Galiano, F., Pelufo-Carbonell, M-J, Peraza-Zurita Y., (2003): 'SEM/EDX and vis spectrophotometry study of the stability of resin-bound mortars used for casting replicas and filling missing parts of historic stone fountains', *Anal Bioanal Chem* **375** 1176–1181

Ruiz-Aggudo, E., Mees, F., Jacobs, P. Rodriguez-Navarro, C., (2007): 'The role of saline solution properties on porous limestone salt weathering by magnesium and sodium sulfates', *Environ. Geol.* **52** 269-281.

Shoval, S., (2003): 'Using FT-IR spectroscopy for study of calcareous ancient ceramics', *Optical materials* **24** 117-122

Saikia, N.J., Sengupta, P., Gogoi, P.K., Borthakura, P.C., (2002): 'Cementitious properties of metakaolin–normal Portland cement mixture in the presence of petroleum effluent treatment plant sludge', *Cement and Concrete Research* **32** 1717–1724

Scherer, G.W., (1999): 'Crystallization in pores', *Cement and Concrete Research* **29** 1347–1358

Scherer, G.W., (2004):'Stress from crystallization of salt', *Cement and Concrete Research* **34** 1613-1624.

Thaulow, N., Sahu, S., (2004): 'Mechanism of concrete deterioration due to salt crystallization', *Materials Characterization* **53** 123– 127

Van Balen, K. and van Gemert, D., (1994): 'Modelling Lime Mortar Carbonation', *Materials and Structures* **27** 393–398.

Van Balen, K., (2005): 'Carbonation reaction of lime, kinetics at ambient temperature', *Cement and Concrete Research* **35** 647– 657

Varas, M.J., Alvarez de Buergo, M., Fort, R., (2005): 'Natural cement as the precursor of Portland cement: Methodology for its identification', *Cement and Concrete Research* **35** 2055 – 2065

Winkler, E.M. and Wilhelm, E.J., (1970): 'Salt burst by hydration pressures in architectural stone in urban atmosphere', *Geol SocAm Bull* **81** 567-571.

Winkler, E.M., Singer, PC, (1972): 'Crystallization pressure of salt in stone and concrete', *Geol SocAm Bull* **83** 3509-3513.

Versión Española

TITULO: ***Mortero de cal hidráulica en el ámbito de la restauración de material pétreo: evaluación de la aplicabilidad***

RESUMEN: *Este estudio presenta los resultados de la aplicación de morteros de cal hidráulica en el ámbito de la conservación y restauración de piedra. Los edificios históricos compuestos por piedra natural, así como esculturas u obras de arte ornamental, expuestos todos ellos a agentes medioambientales, sufren una alteración / degradación severa con el paso del tiempo. Por este motivo, las propiedades físico-químicas de los morteros de cal hidráulica han sido comparados con las de dos rocas calcareníticas (Barxeta y Bateig azul), muy comunes en monumentos históricos valencianos.*

Se estableció un método de procedimiento analítico sistemático en una serie de muestras para probar la compatibilidad / sustituibilidad de las calizas. Las muestras fueron sometidas a las pruebas estándar de envejecimiento físico-químico acelerado. Se han realizado ensayos de resistencia a la compresión y a la flexión en los morteros y el material pétreo con el fin de determinar la degradación física. La alteración por ataque químico se simuló mediante una cámara de SO2 y la prueba de cristalización de sales.

Los experimentos realizados muestran que los morteros ensayados tienen por un lado una resistencia física similar pero por el otro presentan mayores propiedades a la resistencia química, especialmente contra la cristalización de sales, si se compara con piedras naturales, y por tanto pueden ser de especial interés para las réplicas.

PALABRAS CLAVE: *mortero de cal hidráulica, propiedades físico-químicas, envejecimiento acelerado, SEM/EDX, Barxeta, Bateig azul*